Chemistry Communication and Chemical Engineering
ce.ccerci.ac.ir
Research Articles

Corresponding Author Email: maleki@iust.ac.ir

Orcid.org/0000-0001-5490-3350

Keywords:
ultrasonic promotion, green heterogeneous nanocatalyst, catalyst, 1*H*-tetrazole derivatives, HNTs modification, humic acid

Synthesis and Characterization of HNTs@Fe_3O_4@HA-Cu Based on Halloysite Nanotubes as a Green, New and Recyclable Nano-catalyst for the Synthesis of 1*H*-tetrazole Derivatives

Kobra Valadi, Zoleikha Hajizadeh and Ali Maleki*

Catalysts and Organic Synthesis Research Laboratory, Department of Chemistry, Iran University of Science and Technology, Tehran 16846-13114, Iran

Abstract: Recently, researches have been directed towards a simple and consistent path to green chemistry. In this study, halloysite nanotubes were modified by Fe_3O_4 nanoparticles, humic acid molecules and copper (HNTs@Fe_3O_4@HA-Cu) for the first time. Next, the chemical structure, crystalline structure, surface morphology, thermal stability and magnetic properties of the catalyst were checked by Fourier transform infrared (FT-IR), X-ray diffraction (XRD), Field Emission-scanning electron microscopy (SEM), vibration sample magnetometer (VSM) and thermogravimetric analysis (TGA). Then, the catalytic performance of the novel and eco-friendly HNTs@Fe_3O_4@HA-Cu nanocatalyst was investigated in the synthesis of tetrazole derivatives as an important heterocyclic compound. The utilization of this nanocatalyst has many advantages including high efficiency, using non-toxic solvent and doing the reaction in the mild condition. Also, this nanocatalyst has some prominent features like easy separation, green, recoverable and reusable, stability, convenient preparation and highly efficient.

Introduction

Click chemistry has been called strategizing in the preparation of non-harmful chemicals.[1-3] Also, click reactions take place by one-pot and its products have many applications in the fields of biomedical and pharmacological.[4,5] The combination of at least two or more primary substances and in the one-pot condition as well as to the preparation of a single product, is named multi-component reactions (MCRs).[6-9] Tetrazole reaction is an important category of MCRs.[10,11] Today, the preparation of heterocyclic tetrazole molecules has been widely considered and used for various fields.[12-17] Therefore, in this regard, providing a method with the ideal conditions, green chemistry according and high efficiency is of great importance. For this reason, various heterogeneous catalysts such as reported works in literature have been tested and reported toward the synthesis of its important class of chemical reactions.[18-21] But, many of the presented works have some difficult conditions such as low efficiency, long time, low recyclability, long reaction and expensive.

Halloysite nanotubes (HNT) is an inorganic natural that due to its advantages such as non-hazardous, inexpensive, high surface area as well as the presence of hydroxyl groups on its surface has received special attention.[22,23] As well as, Today, Fe_3O_4 nanoparticles have attracted much attention because of their easy and inexpensive synthesis method and more importantly their ability to be separated by magnetic fields.[24-26] On the other, on the other hand, Humic acid (HA) can be combined with metal ions as well as organic and inorganic substrates due to their -OH and -COOH functional groups on its surface.[27-32] In this regard, the design of a novel and environment-friendly nanocatalyst has been suggested. The performance of HNTs@Fe_3O_4@HA-Cu nanocatalyst was checked in the synthesis of heterocycles 1*H*-tetrazole derivatives **4a-j**, by the reaction of benzaldehyde derivatives **1**, malononitrile **2** and sodium azide **3** (Scheme **1**).

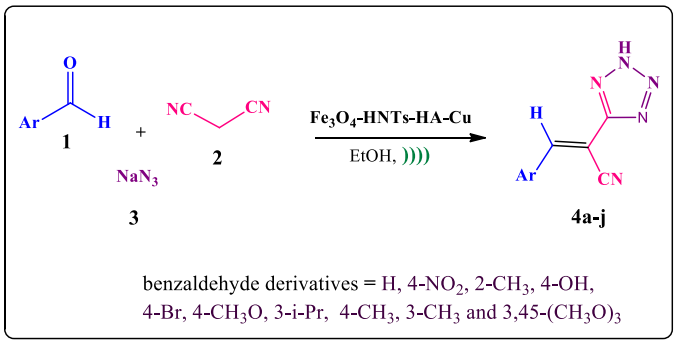

Scheme 1. Catalytic application in the synthesis of 1*H*-tetrazole derivatives **4a-j**

Experimental

General

All of the inorganic, organic chemicals and solvents used in this work including Benzaldehyde (C_7H_6O, ≥99%), 4-Hydroxybenzaldehyde ($C_7H_6O_2$, 98%), 4-Nitrobenzaldehyde ($C_7H_5NO_3$, 98%), 4-Bromobenzaldehyde (C_7H_5BrO, 97%), 4-Methoxybenzaldehyde ($C_8H_8O_2$, 98%), 2-Methylbenzaldehyde (C_8H_8O, 98%), 3-Methylbenzaldehyde

(C_8H_8O, 98%), 4-Methylbenzaldehyde (C_8H_8O, 98%), 3-Isopropylbenzaldehyde ($C_{10}H_{12}O$, 98%) and 3,4,5-Trimethoxybenzaldehyde ($C_{10}H_{12}O_4$, 98%), Sodium hydroxide (NaOH, 97%), Ethanol (C_2H_5OH, 97%), Sodium azide (NaN_3, 99%) and halloysite nanotubes were supplied from Merck and Sigma. Ultrasonic irradiation was performed in an ultrasound cleaning bath KQ-250 DE with a frequency of 40 kHz and power of 250 W. The first test is the melting point measurement, which is measured using the device with Electrothermal 9100 apparatus. FT-IR spectroscopy was achieved by the Shimadzu IR-470 spectrometer and KBr pellets and the resulting diagrams were obtained. EDX analysis was examined with Numerix DXP–X10P device. FE-SEM analysis images are recorded with a Sigma-Zeiss microscope with an attached camera. XRD analysis with the JEOL JDX–8030 (30 kV, 20 mA) device was taken from the samples. Lakeshore 7407 device was applied for VSM analysis. Finally, TGA analysis is registered with an STA504 device.

Preparation of the superparamagnetic nanostructure

Synthesis of HNTs@Fe_3O_4

In the first step, 50 mL of deionized water was added to a mixture of 0.50 g HNTs, 1.60 g $FeCl_3.6H_2O$ and 1.00 g $FeCl_2.4H_2O$ and the aqueous mixture was stirred at room temperature for 30 min. In the second step, the reaction temperature was slowly increased to 80 ˚C. Then, 7.5 mL of NH_3 (ammonia) solution was added drop by drops to reaction mixture. The reaction was placed in the preceding reaction condition for 2 h. Finally, the black product was washed with excess deionized water and dried in an oven at 80 ºC. HNTs@Fe_3O_4 black precipitation was named **(1)**.

Synthesis of HNTs@Fe_3O_4@HA-Cu nano-catalyst

In a 250 mL flask, 0.5 g of **(1)** black precipitate and 0.5 g of humic acid powder were dispersed in the deionized water and stirred at ambient temperature for 24 h. The synthesis nanocomposite was separated by an external magnet and washed several times with ethanol and water. Next, dried by using an oven for 24 h. This black powder was called **(2)**.

HNTs@Fe_3O_4@HA-Cu nanocatalyst

The loading of copper on the prepared HNTs@Fe_3O_4@HA nanocatalyst was done by adding 0.5 g of (2) nanocomposite, 0.5 g of $CuSO_4 \cdot 5H_2O$ powder and 100 mL deionized water in a 250 flask. The mixture was stirred for 24 h at room temperature. The final magnetic nanocomposite was assembled and washed with water for 5 times. HNTs@Fe_3O_4@HA-Cu nanocatalyst was reached by drying at 100 ºC for 3h.

General procedure for the synthesis of tetrazole derivatives 4a-n in the presence of the clay nanostructure catalyst

First, 1.10 mmol of malononitrile, 1.00 mmol of benzaldehyde derivatives and 1.00 mmol of sodium azide with 0.03 g of the favorable catalyst were dispersed in ethanol polar solvent by ultrasonic. Then, the progress of the reaction was investigated by taking TLC (Thin-layer chromatography) from the solution of the reaction vessel. After separating the magnetic nanocatalyst by external fields, the solution of HCL (2N) was added dropwise to the reaction mixture. The pure precipitate of the tetrazole compound was filtrated and dried at 70 ºC.

Results and discussion

In this study, magnetic halloysite nanotubes were modified by HA and Cu as a environment-*friendly*, efficiently and recyclable nanocatalyst for the first time. Then, the successful formation of the nanocomposite was confirmed by the FT-IR, EDX, XRD, SEM, VSM, and TGA analysis. Next, its catalytic ability was evaluated in the synthesis of heterocycles1*H*-tetrazole reactions.

Characterization of HNTs@Fe_3O_4@HA-Cu nano-catalyst

Fourier transform infrared (FT-IR) spectroscopy

To study the functional groups and interactions within the precursors, the FT-IR spectra of HNTs, HNTs@Fe_3O_4@HA, HNTs@Fe_3O_4@HA-Cu and recycle HNTs@Fe_3O_4@HA-Cu were taken. The results are shown in **Fig. 1.** Following absorption spectrum of natural HNTs powder, the peaks appearing in 523, 470, 915 cm^{-1} are related to the stretching vibrations, Al-O-Si, Si-O-Si, Al-OH, respectively. As well as in all spectra, the strong peak appeared at 3400 cm^{-1} coming from the O-H stretching vibrations of HNTs and HA. The bands at 1710 and 1631 cm^{-1} are related to the symmetric and asymmetric vibrations of the carbonyl groups of HA.

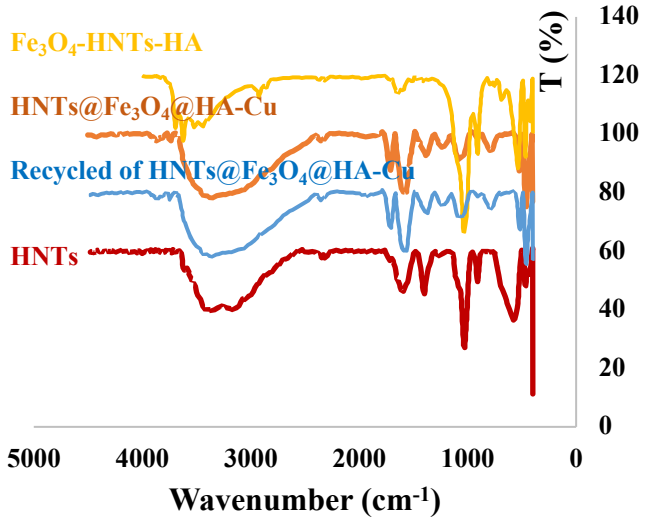

Fig. 1. The FT-IR spectra of HNTs, HNTs@Fe_3O_4@HA and HNTs@Fe_3O_4@HA-Cu and recycled of HNTs@Fe_3O_4@HA-Cu nanocatalyst

Energy-dispersive X-ray (EDX)

The qualitative EDX analysis of the nanocomposite, before and after loading of Cu, were shown in **Fig. 2.** As can be seen in **Fig. 2a,** the synthesis of HNTs@Fe_3O_4@HA nanocomposite was verified by the presence of elements including iron, carbon, silicon, aluminum and oxygen. Moreover, the existence of copper in addition to the presence of O, C, Al, Si, and Fe elements indicate that the Cu is well loaded on HNTs@Fe_3O_4@HA nanocomposite.

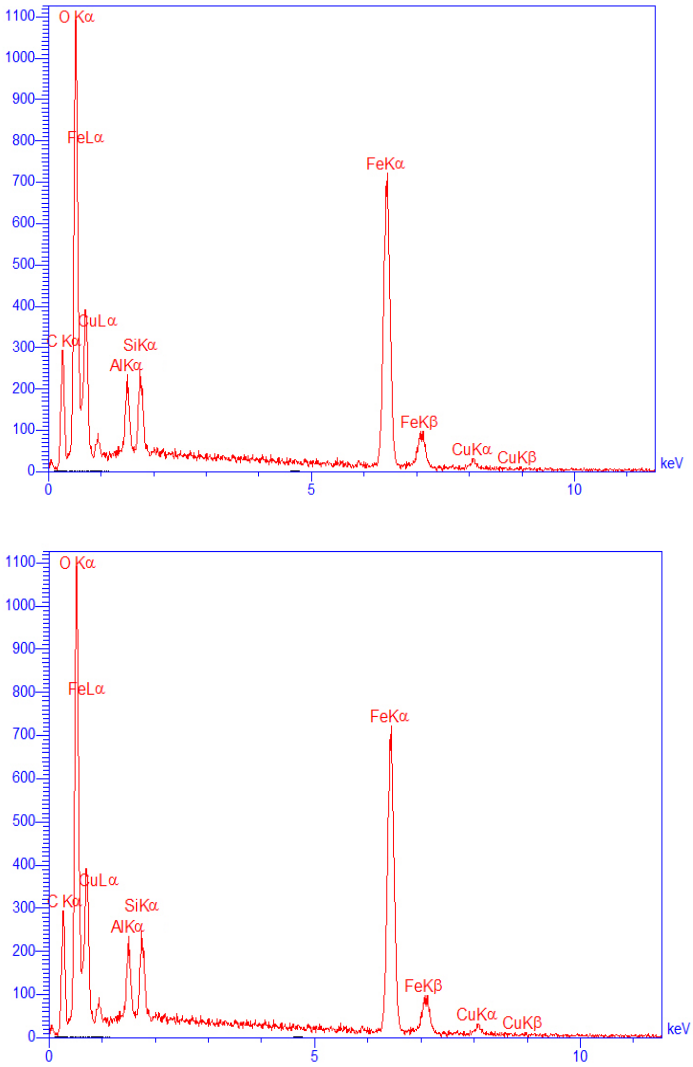

Fig. 2. EDX analysis of a) before and b) after loading of Cu on the HNTs@Fe_3O_4@HA nanocatalyst

X-ray diffraction (XRD)

The HNTs@Fe_3O_4@HA-Cu nanocatalyst with crystalline structure was identified by the XRD pattern (Fig. 3). According to articles, peaks appear at angles (2θ) of 30.24, 35.57, 43.34, 57.21 and 62.71 degrees are related to the Fe_3O_4 nanoparticles. Also, the peaks at angles 43.26 (1 1 1), 53.26 (2 0 0) and 74.50 (2 2 0) indicate the loading of the copper on the HNTs@Fe_3O_4@HA nanocomposite.

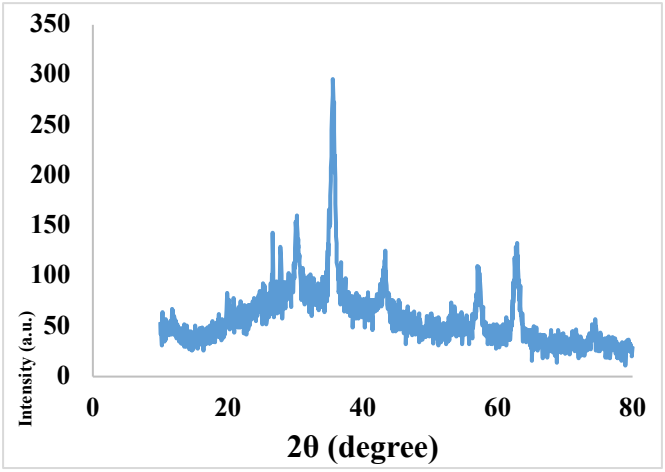

Fig. 3. The XRD pattern of HNTs@Fe_3O_4@HA-Cu nanocatalyst

Field emission-scanning electron microscopy (FE-SEM)

In **Fig. 4**, surface morphology as well as the size of nanoparticles in the HNTs@Fe_3O_4@HA-Cu nanocatalyst was investigated via the FE-SEM image. As expected, the tubular structure of the halloysite was recognized clearly. Meanwhile, the loading of Fe_3O_4 NPs, HA and Cu were well incorporated on the HNTs by some roughness in the figure. Too possible aggregation of the particles in the produced materials are easily recognized in the figure.

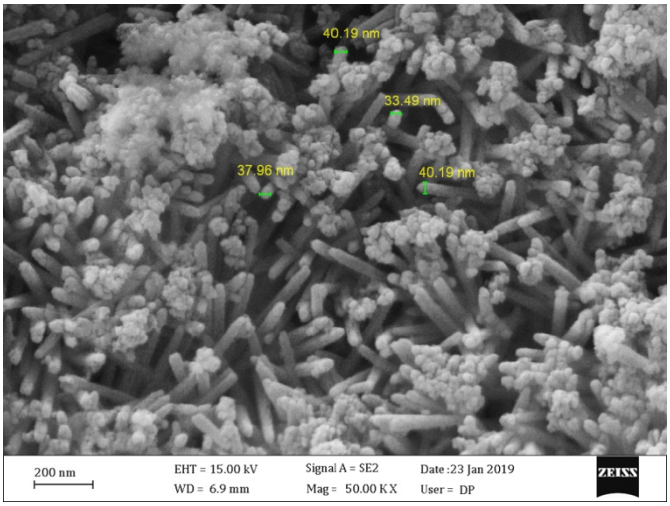

Fig. 4. The FE-SEM image of HNTs@Fe_3O_4@HA-Cu nanocatalyst

Vibrating sample magnetometer (VSM)

Due to the importance of the easy separation and reusing of the nanocatalyst, the magnetic property of the HNTs@Fe_3O_4, HNTs@Fe_3O_4@HA, and HNTs@Fe_3O_4@HA-Cu samples were examined by VSM analysis (Fig. 5). The magnetic property of the HNTs@Fe_3O_4, HNTs@Fe_3O_4@HA and HNTs@Fe_3O_4@HA-Cu were appeared at 30.45, 27.56 and 15.82 emu/g, respectively. As can be seen, the loading of HA, and Cu into the HNTs@Fe_3O_4 nanocomposite leads to the decrease of the magnetic properties in the final nanocomposite. Which is completely consistent with reality and it also

confirms the results of other analyzers. It also confirms the results of other analyzers.

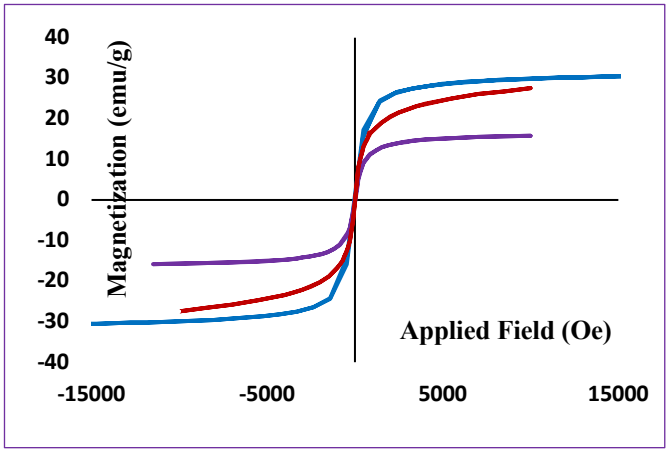

Fig. 5. VSM diagrams of the a) HNTs@Fe_3O_4, b) HNTs@Fe_3O_4@HA and c) HNTs@Fe_3O_4@HA-Cu samples

Thermogravimetric analysis (TGA)

The thermal stability of the HNTs@Fe_3O_4, HNTs@Fe_3O_4@HA and HNTs@Fe_3O_4@HA-Cu nanocomposites were investigated at a temperature range of 20-600 °C (rate = 10 °C/min) and the results were shown in Fig. 6. In all samples a small losing weight is observed below 200 °C due to the evaporation adsorbed moisture. Subsequent losing weight occurred at the range 300-480 °C, is related to the functional groups of HA and HNTs. According to the diagrams that were taken, an intense weight loss appeared in the 350-450 area for HNTs@Fe_3O_4@HA and HNTs@Fe_3O_4@HA-Cu samples are observed that is due to the degradation of the HA structure.

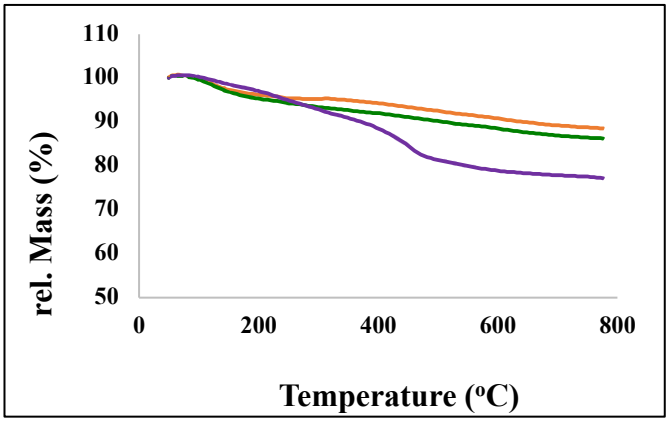

Fig. 6. TGA diagrams of the a) HNTs@Fe_3O_4, b) HNTs@Fe_3O_4@HA and HNTs@Fe_3O_4@HA-Cu samples

Optimization of different parameters in the synthesis of 1*H*-tetrazole derivatives

To obtain the best conditions for the 1*H*-tetrazole reaction, 11 tests with different conditions were performed, and the final results are summarized in **Table 1**. As can be seen when the tetrazole reaction precursor was examined in the absence of catalyst, room temperature, solvent-free and water-free, respectively (**entry 1**). Also, the reflux condition was checked, but the yield was negligible (**entry 2**). The trace yield was obtained in the solvent-free and catalyst-free conditions (**entry 3**). In the next step, reaction with free catalyst conditions was carried out without temperature in the EtOH solvent and the results indicated that the efficiency was still low (**entry 4**). In the next step, the reaction was tested in the presence of ethanol, with ultrasonic waves but in the absence of a catalyst, and this time the efficiency was improved (**entry 5**). For this reason, the other tests of the optimization were examined under ultrasonic irradiation, at 60 °C and ethanol solvents. In this regard 10, 20, 30, 40, 50 and 60 mg of HNTs@Fe_3O_4@HA-Cu nanocatalyst was used and the best efficiency (98%) was observed for the reaction using 30 mg of catalyst (**entry 6-10**). In the end, the reaction, with 11 conditions, but the Dimethylformamide solvent was tested, but the reaction yield is lower than the same condition (**entry 11**).

Table 1. Optimization of the model reaction conditions

Entry	Solvent	Amount of catalyst (mg)	Temp. (°C)	Time (min)	Yield (%)
1	Solvent-free	-	r.t.	100	Trace
2	Water	-	r.t.	100	Trace
3	Solvent-free	-	Reflux	100	Trace
4	Ethanol	-	r.t.	100	Trace
5	Ethanol	-	Ultrasonic	40	55
6	Ethanol	20	Ultrasonic	40	95
7	Water-Ethanol	30	Ultrasonic	40	97
8	Ethanol	40	Ultrasonic	40	96
9	Ethanol	50	Ultrasonic	40	94
10	Ethanol	60	Ultrasonic	40	90
11	Dimethylformamide	30	Ultrasonic	40	95

To confirm and extend the catalytic performance of HNTs@Fe_3O_4@HA-Cu, 10 different tetrazole derivatives with optimized conditions were synthesized and reported (**Table 2**).

Table 2. Synthesis of 1*H*-tetrazole derivatives **4a-j** under optimized conditions.

Entry	Aldehyde	Product	Time (min)	Yield (%)	M.P (°C)	
					Found	Reported [Ref.]
1	Benzaldehyde	**5a**	9	97	170-171	168-170 [33]
2	4-Nitrobenzaldehyde	**5b**	10	93	167-169	166-168 [33]
3	4-Bromobenzaldehyde	**5c**	10	90	248-250	165-167 [33]
4	4-Hydroxybenzaldehyde	**5d**	10	88	160-162	159-161 [33]
5	2-Methybenzaldehyde	**5e**	7	94	158-159	157-159 [34]
6	4-Methoxybenzaldehyde	**5f**	8	87	153-154	153-154 [34]
7	4-Isopropylbenzaldehyde	**5g**	10	92	127-128	128-130 [34]
8	4-Methybenzaldehyde	**5h**	10	88	190-192	189-191[34]
9	3-Methylbenzaldehyde	**5i**	10	95	207-209	130-132 [34]
10	3,4,5-Trimethoxybenzaldehyde	**5j**	10	98	157-159	Present

Proposed mechanism

The proposed mechanism for the interaction between raw materials (benzaldehyde derivatives, malononitrile and sodium azide) in the presence of the nano-catalyst was plotted in the synthesize of tetrazole derivatives (**Scheme 2**). Via the knoevenagel condensation between aldehyde derivatives **1** and malononitrile **2**, the intermediate **I** was obtained. Next, intermediate **II** was formed by the reaction of the intermediate **I** and sodium azide **3**. After that, the intermediate **III** was achieved by [2+3] cycloaddition reactions of heterocyclic compounds. Due to exchange Cu with H in the final products (**4a-j**), the hydrochloric acid was added in the final process.

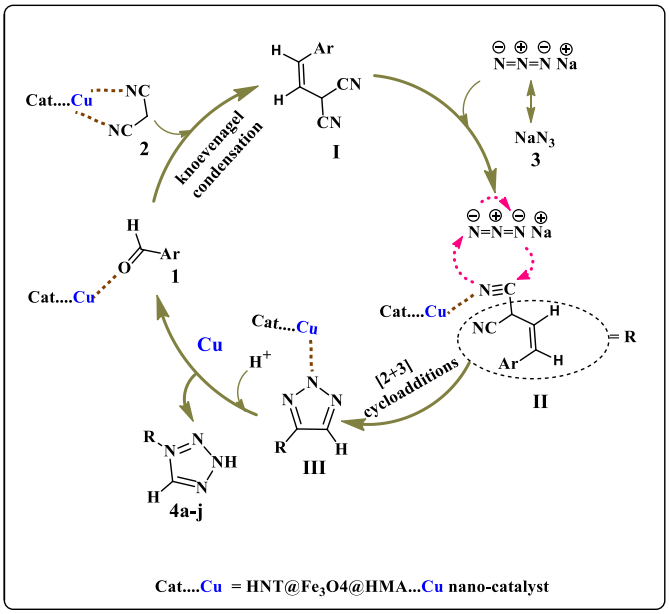

Scheme 2. Proposed mechanism for the synthesis of **4a-j** by HNT@Fe_3O_4@HA-Cu nanocatalyst

Catalyst recyclability test

One of the most important parameters of catalysts is their recyclability and ultimately their easy separation from the reaction medium without reducing its catalytic activity. For this reason, as shown in **Fig. 7**, after the reaction was completed, the recycled catalyst was tested 10 times and the efficiency of the synthesized products was evaluated. The experimental results show a no significant change in the catalytic activity and the yield of synthesized products were in this article, in addition to using green solvent, short reaction time and high efficiency, as can be seen in the recycling diagram(Fig.) the nanocatalyst is highly recyclable without losing catalytic activity.

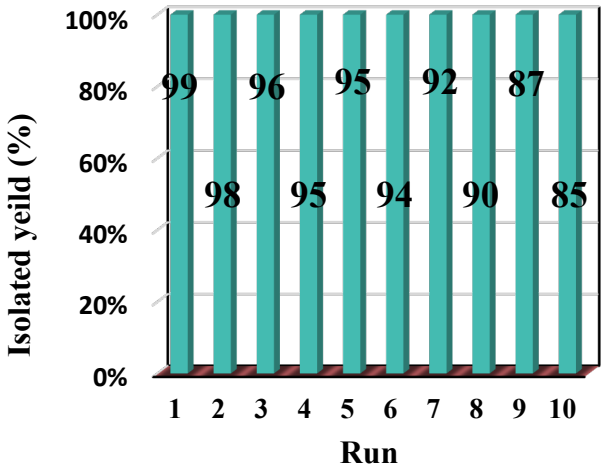

Fig. 7. Recycling diagram of new HNTs@Fe_3O_4@-HA-Cu nanocatalyst for **4a**

Conclusions

In summary, the HNTs as a matrix were used, because of its abundant hydroxyl functional groups, environment-friendly and easy to access. The synthesized HNTs@Fe_3O_4@HA-Cu nanocatalyst was developed that incorporates all the properties of the raw materials. As can be seen in Fig. 1-6, the functional groups and interaction of the between materials, structural property, elements present and magnetic properties as well as the thermal stability of the new HNTs@Fe_3O_4@HA–Cu nanocatalyst were investigated and confirmed by FT-IR, EDX, SEM, XRD, VSM and TGA, analyses, respectively. In the next step, the catalytic performance of the HNTs@Fe_3O_4@HA–Cu nanocatalyst for the 1*H*-tetrazole reaction, by condensation of benzaldehyde derivatives, malononitrile and sodium azide, was tested. As expected in accordance with Table 1, after optimizing the parameters affecting the reaction efficiency, 12 derivatives of the 1*H*-tetrazole reaction were synthesized and in Table 2, and the best efficiency was reported for the 5n derivative. In addition to the cases mentioned in Fig. 7, the nanocatalyst recycling ability was repeated 8 times, and it was observed that the new green HNTs@Fe_3O_4@HA-Cu nanocatalyst catalyst retained its catalytic performance over several steps and as can be seen, the efficiency of the synthesized derivatives did not decrease significantly.

Acknowledgement

The authors thank the Iran University of Science and Technology (IUST) for partial financial support by the Research Council and the reviewers for their valuable comments and suggestions.

Conflicts of interest

There are no conflicts to declare.

References

1. Aureggi, V.; Sedelmeier, G. 1, 3-Dipolar Cycloaddition: Click Chemistry for the Synthesis of 5-substituted

tetrazoles from Organoaluminum Azides and Nitriles. *Angew. Chem. Int*, **2007**, 46, 8440-8444.

2. S.G. Pharande, M.A. Renterla-Gomez, R.Gamez-Montano, J. Name. 00 (2013) 1-3.

3. Ol'shevskaya, V.A.; Makarenkov, A.V.; Borisov, Y.A.; Ananyev, I.V.; Kononova, E.G.; Kalinin, V.N.; Ponomaryov, A.B.; CAN Catalysis and Click Chemistry Routes in the Synthesis of Carborane Containing Ferrocenes. *Polyhedron*, **2018**, 141, 181-190.

4. Zowska, J.G.; Boratynski, P.J.; Kowalczyk, R.; Lipke, K.; Czapor-Irzabek, H. Copper (II) Complexes of Chiral 1,2,3-triazole biheterocyclic Click Ligands Equipped in Cinchona Alkaloid Moiety. *Polyhedron*, **2017**, 121, 1-8.

5. Maleki, A.; Rahimi, J.; Valadi, K. Sulfonated Fe3O4@PVA superparamagnetic nanostructure: Design, in-situ preparation, characterization, and application in the synthesis of imidazoles as a highly efficient organic-inorganic Bronsted acid catalyst. *Nano-Struct. Nano-Objects*, **2019**, 18, 100264.

6. A. Maleki, RSC Adv. 4 (2014) 64169-64173.

7. Maleki, A. One-pot multicomponent synthesis of diazepine derivatives using terminal alkynes in the presence of silica-supported superparamagnetic iron oxide nanoparticles. *Tetrahedron Lett*, **2013**, 54(16), 2055-2059.

8. Jafari Chermahini, Z.; Najafi Chermahini, A.; Dabbagh, H.A.; Teimouri, A. One-pot synthesis of ethyl-3-aryl-2-(1H-tetrazol-5-yl)acrylates and 3-(1H-tetrazol-5-yl)coumarins via tandem [2+3] dipolar cycloaddition reaction-Knoevenagel condensation. ChemistrySelect, **2016**, 1(3), 430-433.

9. Gerhards, H.; Krest, A.; Eulgem, P.J.; Naumann, D.; Rokitta, D.; Valldor, M.; Klein, A. Synthesis and coordination chemistry of perfluoroaryl -1H-tetrazoles. Polyhedron, **2015**, 100, 271-281.

10. Ishihara, K.; Shioiri, T.; Matsugi, M. Stereospecific synthesis of 1,5-disubstituted tetrazoles from ketoximes via a Beckmann rearrangement facilitated by diphenyl phosphorazidate. *Tetrahedron Lett*, **2019**, 60, 1295-1298.

11. Hou, X.; Guo, Z.; Yang, L.; Ma, H. Four three-dimensional metal-organic frameworks assembled from 1H-tetrazole: synthesis, crystal structure, and thermal properties. *Polyhedron*, **2019**, 160, 198-206.

12. Teimouri, A.; Chermahini, A.N. Zeolite and sulfated zirconia as catalysts for the synthesis of 5-substituted 1H-tetrazoles via [2+3] cycloaddition of nitriles and sodium azide. *Polyhedron*, **2011**, 30, 2606-2610.

13. Kundu, D.; Majee, A.; Hajra, A. Indium triflate-catalyzed one-pot synthesis of 1-substituted 1H-1,2,3,4-tetrazoles under solvent-free conditions, *Tetrahedron. Lett*, **2009**, 50, 2668-2670.

14. Heravi, M.M.; Fazeli, A.; Oskooie, H.A.; Beheshtiha, Y.S.; Valizadeh, H. Click synthesis of 5-substituted 1H-tetrazoles from aldehydes, hydroxylamine, and [bmim] N_3 via one-pot, three-component reaction. *Synlett*, **2012**, 23, 2927-2930.

15. Tamoradi, T.; Taherabadi, S.; Ghadermazi, M. Neodymium immobilized on Fe_3O_4: a new and recoverable catalyst for oxidation reactions and synthesis of 5-substituted 1H-tetrazoles in green condition. *Polyhedron*, **2019**, 171, 305-311.

16. Fazeli, A.; Oskooie, H.A.; Beheshtiha, Y.S.; Heravi, M.M.; Valizadeh, H.; Bamoharram, F.F. Heteropolyacid catalyzed click synthesis of 5-substituted 1H-tetrazoles from [bmim]N3 and nitriles under solvent-free conditions. *Monatsh. Chem*, **2013**,144, 1407-1410.

17. Patil, V.S.; Nandre, K.P.; Borse, A.U.; Bhosale, S.V. InCl3-catalysed [2+3] cycloaddition reaction: A rapid synthesis of 5-substituted 1H-tetrazole under microwave irradiation. *Journal of Chemistry*, 2012, 9, 1145-1152.

18. Epishina, M.A.; Kulikov, A.S.; Ignat'ev, N.V.; Schulte, M.; Makhova, N.N. Ionic liquid-assisted synthesis of 5-mono and 1,5-disubstituted tetrazoles. *Mendeleev Commun.* **2011**, 21, 334-336.

19. Voitekhovich, S.V.; Grigoriev, Y.V.; Lyakhov, A.S.; Matulis, V.E.; Ivashkevich, L.S.; Ivashkevich, O.A. 2-(1H-tetrazol-1-yl) thiazole: complexation and copper-assisted tetrazole ring transformation. *Polyhedron*, **2019**, 171, 423-432.

20. B. Gutmann, J.P. Roduit, D. Roberge, C.O. Kappe, Int. Ed. 49 (2010) 7101-7105.

21. Bonnamour, J.; Bolm, C. Iron salts in the catalyzed synthesis of 5-substituted 1H-tetrazoles. *Chem. Eur. J,* **2009**, 15, 4543-4545.

22. Massaro, M.; Colletti, C.G.; Buscemi, G.; Cataldo, S.; Guernelli, S.; Lazzara, G.; Liotta, L.F.; Parisi, F.; Pettignano, A.; Riela, S. Palladium nanoparticles immobilized on halloysite nanotubes covered by a multilayer network for catalytic applications. *New J. Chem***,** **2018,** 42, 13938-13947.

23. Jinhua, W.; Xiang, Z.; Bing, Z.; Yafei, Z.; Rui, Z.; Jindun, L.; Rongfeng, C. Rapid adsorption of Cr (VI) on modified halloysite nanotubes. *Desalination*, **2010**, 259, 22-28.

24. Massaro, M.; Lazzara, G.; Milioto, S.; Notoa, R.; Riela, S. Covalently modified halloysite clay nanotubes: synthesis, properties, biological and medical applications. *J. Mater. Chem. B*, **2017**, 5, 2867-2882.

25. Jiang, W.; Cai, Q.; Xu, W.; Yang, M.; Cai, Y.; Dionysios, D.; OShea, K.E. Cr (VI) adsorption and reduction by humic acid coated on magnetite. *Environ. Sci. Technol*, **2014,** 48, 8078-8085.

26. Zhang, Y.J.; Duan, Z.K.; Yin, Z.J.X. *Colloids Surf. A*, **2015**, 481, 108-116.

27. Lippold, H.; Eidner, S.; Kumke, M.U. Dynamics of metal-humate complexation equilibria as revealed by isotope exchange studies_a matter of concentration and time. *Journal of Geochim. Cosmochim. Acta*, 2017, 197, 62-70.

28. Caceres-V elez, P.R.; Fascineli, M.L.; Sousa, M.H.; Grisolia, C.K.; Yate, L.; de Souza, P.E.N.; Estrela-Lopis, I.; Moya, S.; Azevedo, R.B. Humic acid attenuation of silver nanoparticle toxicity by Ion complexation and the formation of a Ag^{3+} coating. *J. Hazard. Mater*, **2018**, 353, 173-181.

29. A. Maleki, R. Taheri-Ledari, M. Soroushnejad, Org. Supramol. Chem. 3 (2018) 13057-13062.

30. Magnacca, G.; Allera, A.; Montoneri, E.; Celi, L.; Benito, D.E.; Gagliardi, L.G.; Gonzalez, M.C.; Martire, D.O.; Carlos, L. Novel magnetic nanoparticles coated with waste-sourced biobased substances as sustainable adsorbing materials. *ACS Sustain. Chem. Eng*, **2014**, 2, 1518-1524.

31. Vatanpoura, V.; Shahsavarifar, S.; Khorshidia, S.; Masteri-Farahani, M. J. A novel antifouling ultrafiltration membranes prepared from percarboxylic acid functionalized SiO_2 bound Fe_3O_4 nanoparticles (SCMNP-COOOH)/polyethersulfone nanocomposite for BSA

separation and dye removal. *Chem. Technol. Biotechnol*, **2019**, 94, 1341-1353.

32. Boruah, P.K.; Sharma, B.; Karbhal, I.; Shelke, M.V.; Das, M.R. Ammonia-modified graphene sheets decorated with magnetic Fe3O4 nanoparticles for the photocatalytic and photo-Fenton degradation of Phenolic compounds under sunlight irradiation. *J. Hazard. Mater*, **2017**, 325, 90-100.

33. Tisseh, Z.N.; Dabiri, M.; Nobahar, M.; Khavasi, H.R.; Bazgir, A. Catalyst-free, aqueous and highly diastereoselective synthesis of new 5-substituted 1H-tetrazoles via a multi-component domino Knoevenagel condensation/1,3 dipolar cycloaddition reaction. *Tetrahedron*, **2012**, 68, 1769-1773.

34. J. Safaei-Ghomi1, S. Paymard-Samani, Chem. Heterocyclic Com. 50 (2015) 1567-1574.